

Second-harmonic imaging of plant polysaccharides

Guy Cox

University of Sydney
Electron Microscope Unit
NSW 2006, Australia
and

Instituto Gulbenkian de Ciência,
PT-2780-156 Oeiras, Portugal
E-mail: guy@emu.usyd.edu.au

Nuno Moreno

José Feijó

Instituto Gulbenkian de Ciência,
PT-2780-156 Oeiras, Portugal

Abstract. The application of second-harmonic generation (SHG) microscopy to plant materials has been neglected hitherto even though it would seem to have promise for identification and characterization of biologically and commercially important plant polysaccharides. We find that imaging of cellulose requires rather high laser powers, which are above optimal values for live cell imaging. Starch, however, is easily imaged by the technique at laser fluences compatible with extended cell viability. This also has useful applications in imaging plant-derived starchy food products. Lignin in plant cell walls shows a strong three-photon excited fluorescence, which may be enhanced by resonance effects. © 2005 Society of Photo-Optical Instrumentation Engineers.

[DOI: 10.1117/1.1896005]

Keywords: second-harmonic generation; polysaccharides; cellulose; starch three-photon fluorescence; food microscopy.

Paper 04062 received Apr. 20, 2004; revised manuscript received Aug. 17, 2004; accepted for publication Aug. 20, 2004; published online Apr. 14, 2005. This paper is based on a paper presented at the SPIE conference on multiphoton microscopy in the Biomedical Sciences IV, Jan. 2004, San Jose, California. The paper presented there appears (unrefereed) in SPIE Proceedings Vol. 5323.

1 Introduction

Polysaccharides have a dual role in plant cells, as long- and short-term storage reserves and as the major structural component of the plant. (Arthropods are the only major animal group to make extensive use of structural polysaccharides, in their chitin-based exoskeletons). Chitin, a polymer of glucosamine, is also found in fungi, but green plants use cellulose, which is found only in one small group of animals, the Tunicata. Both storage and structural polysaccharides of plants are of enormous practical and economic use to humankind.

The plant cell wall consists of a matrix of more or less amorphous polysaccharides (glucans, mannans, and arabinans) reinforced by microfibrils of highly crystalline cellulose, a β 1:4 linked glucan.¹ The arrangement and orientation of the cellulose microfibrils is important both for the function of the individual cell and the development of the plant as a whole.^{2,3} In woody tissues, the structure is given further resistance and rigidity by impregnation with lignin, a phenolic compound. Cell walls are critical for plant structure and function and also provide the base of the food chain for the animal kingdom. They are the raw material for many human industries such as timber, fabric, and paper, all products whose characteristics ultimately depend on the arrangement of cellulose microfibrils.

Plants store polysaccharides (usually starch) as long-term energy and carbon reserves in a wide variety of organs such as seeds and tubers. These are of fundamental importance to the human diet, and hence of major economic importance. Starch is also stored on a temporary basis in leaves—in most plants it is the first major product of photosynthesis and accumulates in the chloroplasts of the photosynthetic tissues during the

day, dwindling during the night. (In the “C4” plants, malic acid is the primary product and is converted to starch only in the leaf chloroplasts which surround the vascular tissues.)^{4,5} Starch, in specialized plastids termed amyloplasts, is also important for geoperception in plant roots.⁶ Starch consists of two forms—amylose, long chains of α 1:4 linked glucose residues, and amylopectin, shorter α 1:4 glucans with branches introduced by α 1:6 linkages. The proportions and properties of these are important in food preparation. Amylose in particular is often highly crystalline and therefore likely to give a second-harmonic signal.

Only a few papers to date have looked at plant cells using second-harmonic generation (SHG). Mizutani et al.⁷ imaged starch grains in living algal cells by SHG, using a pulsed neodymium laser in a wide-field microscope with a CCD camera. This approach is not depth-selective and hence discards one of the chief benefits of SHG microscopy, the ability to carry out 3-D imaging.^{8,9} It also requires a laser working at 1064 nm or longer for the image to be at a wavelength for which the objective is corrected. The one benefit is that the resolution is determined by the wavelength of the harmonic not the fundamental, but given the shorter wavelength of a titanium sapphire (Ti-S) laser, and the superresolution given by nonlinear excitation,¹⁰ scanned microscopy will in practice not be significantly worse in resolution.

Chu et al.¹¹ used a stage-scanning microscope and generated 3-D harmonic images of plant cells using a chromium forsterite laser at 1230 nm. They found that the very long excitation wavelength greatly reduced tissue autofluorescence, facilitating the detection of weak signals. They showed images of cell walls, reporting that they could obtain an SHG signal from cellulose, as well as from starch grains in the chloroplasts. They further suggested that chloroplast thylakoid

Address all correspondence to Professor Guy Cox, University of Sydney, Electron Microscope Unit, F09, Sydney, NSW 2006, Australia

membranes (the stacks of membranes that perform photosynthesis) also gave an SHG signal. Both these papers^{7,11} presented only low-magnification images in which high resolution was not achieved.

Because of the commercial importance of both cellulose fibers and starch, novel imaging methods that can give information about structure, crystallinity, and orientation could have wide applicability. Here, we investigate SHG imaging of both living plant cells and starch-containing plant products. Rather than the 1- to 1.2- μm wavelengths used previously,^{7,11} we used a shorter wavelength titanium sapphire laser that is also suitable for two-photon fluorescence (TPF) imaging, at wavelengths between 800 and 850 nm. This brings the harmonic into the range of 400 to 425 nm, where it is still readily transmitted, but lenses are typically not well corrected; since the optics of the collection lenses play no part in the imaging process, this is not an issue.

2 Materials and Methods

2.1 Plant Materials

Stems of *Lantana camara* were collected from the garden of the Instituto Gulbenkian de Ciência, sectioned by hand, and mounted in water. Petioles of celery (*Apium graveolens*) were purchased commercially and also sectioned freehand and mounted in water. Some collenchyma ribs from the celery petioles were stripped and mounted on large coverslips on the stage of the inverted microscope in surplus water, so that the cellulose fiber orientation would be transverse to the optic axis. Moss (unidentified species) was collected from a wall in Sydney and fronds with two or three leaflets were examined entire in water.

Rice grains (*Oryza sativa*), were crudely hand sectioned and mounted in immersion oil so that the starch did not become hydrated. Three varieties were used: Thai jasmine (long grain), Thai glutinous (short grain), and Italian arborio. Rice-flour-based starch and starch/lipid pastes of the type used in food production were supplied by Professor Les Copeland and Ms. Chiming Tang at the University of Sydney.

2.2 Microscopy

At the Instituto Gulbenkian de Ciência (IGC), the microscope used was a Bio-Rad MRC1024ES MP confocal microscope, equipped for multiphoton microscopy with a Coherent Verdi-Mira 900f Ti-S femtosecond-pulsed laser and dual-channel nondescanned detectors, mounted on a Nikon Eclipse TE300 inverted microscope. Plan-Apo 20 \times numerical aperture (NA) 0.75 dry and 40 \times NA 1.3 oil-immersion lenses were used. A 0.85 NA condenser was fitted. For the fluorescence signal, we used the external detectors with a D525/50-nm bandpass filter and a 550-nm 50 DCLP dichroic together with a bandpass filter HQ575/150 nm. A transmission detector was not available at the time, and the second-harmonic (SH) images were collected in the backward direction using 840-nm excitation with a bandpass filter D390/70.

In Sydney a Leica DMIRBE inverted microscope, fitted with a Leica TCS-SP2 spectrometric confocal head (Leica Microsystems, Heidelberg, Germany), was used. The laser is a Coherent Mira titanium-sapphire system, tunable between 700 and 1000 nm, operating in the femtosecond regime and pumped by a 5-W Verdi solid-state laser (Coherent Scientific,

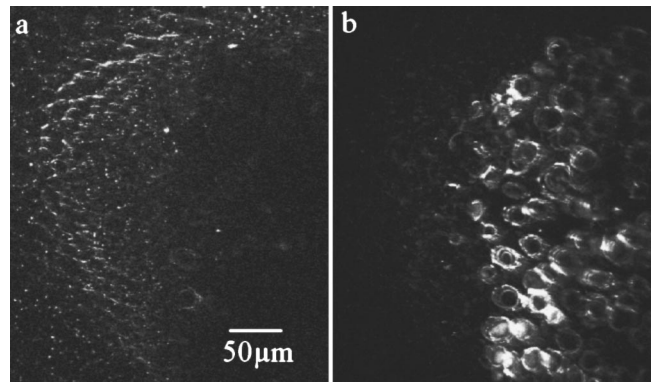


Fig. 1 Collenchyma cells in the bundle cap of celery petiole, hand section imaged in the transmission direction: (a) SHG image in which only the very cellulose rich collenchyma cells are visible and (b) broadband fluorescence image (500 to 600 nm) showing the autofluorescence of the lignin in the spirally thickened tracheids, but no signal in the bundle cap; $\times 20$ NA 0.5 dry objective.

Santa Clara, California). All additional detectors and optical equipment were supplied by Leica Microsystems, with the exception of the additional filters and dichroics, supplied by Chroma Inc (Brattleboro, Vermont). The setup was as described previously.^{9,12} We used 830-nm illumination with a 415/10-nm detection barrier filter in one of the two transmission channels to collect the SH.

3 Results

3.1 Cellulose

The celery petiole has substantial bundles of collenchyma cells, located both in subepidermal bundles (ribs) and adjacent to the vascular bundles (bundle caps). Collenchyma walls were chosen as a useful test sample since they are very rich in cellulose and are nonfluorescent, being entirely unlignified. The only substantial fluorescence signal in these cells comes from the chloroplasts, which are not numerous. Both in transmission and backscattered mode we saw only a very weak SHG signal using maximum laser power. Figure 1 shows a transverse section of a celery petiole imaged in both SHG and fluorescent mode. The collenchyma cells of the bundle cap are visible only in the SHG image, while the lignified tracheid walls show strong two-photon-excited fluorescence and very little SH. The orientation-dependent nature of the SHG imaging process is revealed by the fact that only walls in one orientation are strongly imaged. This was taken on the Leica, using the transmission detector, and it was necessary to average 16 frames for an adequate SNR.

To investigate the orientation dependence of the signal, longitudinal arrays of cells were required, since the orientation of the cellulose microfibrils in these cells is predominantly along the long axis of the cells.^{13–15} For this purpose, entire collenchyma bundles (ribs) were stripped from the petiole and placed in water on a large coverslip on the inverted microscope (Nikon/Bio-Rad) and imaged in backscattered mode. Transmitted SHG detection is not practicable with such a thick specimen.

Figure 2 shows the result. The strongest signal is seen when the longitudinal walls are at 90 deg to the direction of

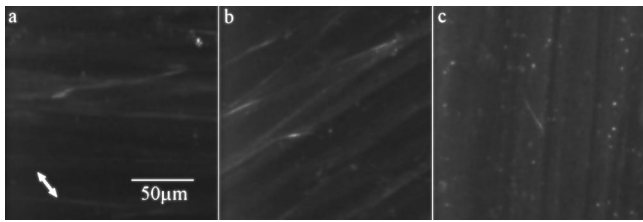


Fig. 2 Collenchyma rib from celery petiole, placed at three different orientations. The double arrow shows the direction of polarization of the 840-nm laser beam: (a) left to right (cellulose fibril orientation 0 deg), (b) 45 deg, and (c) up to down (90 deg); $\times 20$ objective.

polarization [Fig. 2(b)]; with the cells at 0 and 90 deg, the strongest signal comes from transverse walls, though in Fig. 2(c) it is a wall parallel to the polarization direction. However, it cannot be assumed that the cellulose fibers in transverse walls necessarily have a microfibril orientation following the wall direction; only the long walls show a strong alignment.

Lantana stems are woody and therefore have lignified fibers but also have collenchyma. As Fig. 3(a) shows, the lignified fibers (f) give a brighter SHG image than the collenchyma (c). The excitation here is at 840 nm, so the SH is at 420 nm and the detected range is 355 to 425 nm. Therefore, two-photon-excited fluorescence should not be detected. However, the middle lamella region is very bright, and this is where the most lignin is present, as is seen in the TPF fluorescence channel [Fig. 3(b)]. This led us to suspect that we might be seeing some three-photon-excited fluorescence in the violet region from lignin. However, the image was orientation dependent, as shown in the inset, which would imply that the signal is in fact the harmonic from cellulose. (While fluorescence can also show orientation dependence in some cases, the fluorescent cell-wall components lignin and cutin are essentially amorphous, so fluorescence from either source should not show any polarization dependence.) Tuning the laser to 870 nm (SH therefore 435 nm) should exclude the

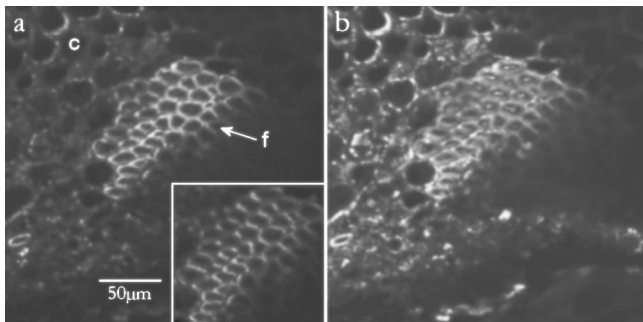


Fig. 3 Transverse section of *Lantana* stem, 840-nm excitation: (a) 355- to 425-nm detection showing a weak signal from the collenchyma (c) and a stronger one from the lignified fibers (f); inset, the fiber bundle rotated ~ 60 deg relative to the excitation (the image has been rotated back to match the main picture); and (b) TPF image for 500- to 650-nm detection. The signal from the fibers seems to be a combination of SHG and three-photon fluorescence; it shows orientation dependence but it matches the TPF signal closely. The bright fluorescence around the collenchyma cells in (b) is from the chloroplasts—punctate SHG signal showing starch grains is seen in (a). $\times 20$ NA 0.5 objective.

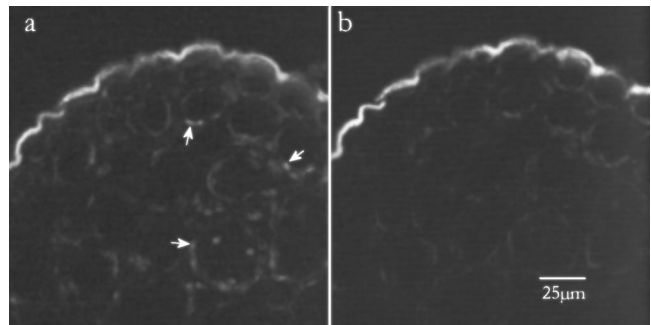


Fig. 4 Epidermis: (a) 840-nm and (b) 870-nm excitation, with detection between 355 and 425 nm. The strong signal from the cuticle does not change with change of excitation wavelength, showing that it is three-photon-excited autofluorescence. The SHG signal from starch grains in the chloroplasts (arrows) disappears at the longer excitation since the harmonic is now at 435 nm and so will not enter the detector; $\times 20$ NA 0.5 objective.

SH; in fact, the image became much dimmer but did not disappear. Both components therefore seem to contribute the image, and it seems possible that there may be some degree of resonant enhancement of fluorescence.

The cuticle of the epidermis showed very strong violet or UV three-photon fluorescence (Fig. 4). In this case, there was little or no change in signal between 840 and 870 nm, so it must be a pure fluorescence image. It is clear that the SH signal is being excluded at 870 nm since starch grains in the chloroplasts (arrowed) are visible at 840 and not at 870 nm.

3.2 Starch

Chloroplasts in celery and *Lantana* showed a signal in the SHG image, which did not colocalize with the autofluorescence of the chlorophyll [Fig. 3(a)], and we attributed this to starch. As a test sample, we used a prepared slide of starch grains (Bio-Rad Microscience, Hemel Hempstead, United Kingdom). Figure 5 shows that these gave a strong SHG signal. Crystalline starch in starch grains is typically organized with the crystallites in a radial fashion, which gives a characteristic cross image in polarized light.¹⁶ This in turn means that the SHG image will be orientation dependent, and Figs. 4(a) and 4(b) shows that this is so—opposite quadrants are bright when the sample is rotated through 90 deg (the images

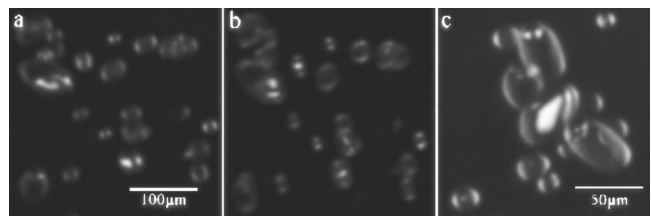


Fig. 5 Prepared slide of starch grains, SHG image excited at 830 nm, detected with a 415/10 narrowband filter (Leica TCS-SP2). (a) and (b) Single plane images of the same area, showing the orientation dependence of the signal. The slide was rotated through 90 deg between the images, which have then been rotated to bring them back to the same position; $\times 10$ objective NA 0.3. (c) Maximum brightness projection from 50 optical sections taken with a higher power objective ($\times 40$ NA 0.75).

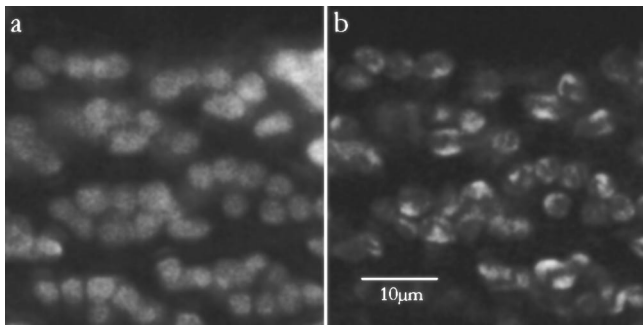


Fig. 6 Living moss leaflet in water, using $\times 63$ NA 0.12 water immersion objective: (a) chlorophyll autofluorescence and (b) SHG. A very low excitation dose was used and a median filter was applied (3×3 kernel) to improve the SNR with minimal effect on resolution.

have been rotated to bring them back to equivalent positions). The signal is strong, and a very low excitation level is adequate for a high-quality image. Figure 5(c) shows a maximum brightness projection from a 50-section stack through this sample, and illustrates the quality of imaging obtainable from a higher NA lens (the limitations of our stage mean that rotation of the sample is feasible only with a low-power objective).

These results encouraged us to believe that we could image starch in living cells at fluences that would not have adverse effects on normal cell physiology. Starch is formed during photosynthesis and therefore it is particularly useful to be able to image starch in leaves that remain photosynthetically competent. However, the leaves of higher plants contain extensive airspaces, which hinder effective imaging. Bryophyte (moss) leaves are more suitable since they have only a single layer of cells over most of the lamina, and therefore no air spaces. Moss leaves do not contain lignin but they do contain substantial amounts of other phenolic compounds,¹⁷ which fluoresce in the blue and green, as well as chlorophyll, fluorescing in the red.

A minimal excitation dose was used in the interest of preserving cell viability and photosynthetic functionality (judged by maintenance of red fluorescence in the chloroplasts). High-magnification images showed excellent resolution in the SHG channel, taken as representing starch in the chloroplasts (Fig. 6). This image was sampled at approximately Nyquist resolution (82-nm pixel size) and therefore represents the limit of resolution for imaging living tissue.

Using a lower zoom value to reduce dose as much as possible, it proved simple to collect 3-D images, as shown in Fig. 7, a $256 \times 256 \times 97$ voxel stack. The green channel showed the cell walls clearly, presumably from autofluorescence of tannins or other phenolics, while the chlorophyll was detected in the second (red) channel of the backscattered detector and the SH in the transmission detector. There was no visible deterioration in the cell after the collection of this data set; in particular, the autofluorescence of the chlorophyll, normally a sensitive indicator of damage, was unchanged.

There are many aspects in which the structure of starch is useful to the food industry, and we therefore investigated the applicability of SHG imaging to these problems. Conventional microscope preparation of starch seeds such as rice grains inevitably leads to the partial hydration of the starch

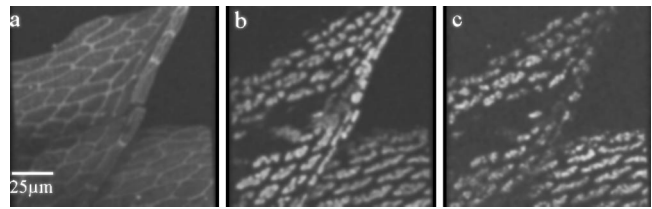


Fig. 7 Living moss leaflets in water; maximum brightness projection from 97 optical sections covering a depth of $44 \mu\text{m}$: (a) green fluorescence from phenolics, (b) red fluorescence from chlorophyll, and (c) SHG at 415 nm. Leica TCS-SP2, $\times 63$ NA 1.2 water immersion objective.

with concomitant swelling and structural changes. We therefore hand cut sections of grains and mounted them in immersion oil. Figure 8(a) shows that a strong signal and a detailed image was obtained but it is not easy to interpret; a more sophisticated preparation technique may be needed to take this approach further.

Starch pastes and doughs of one sort or another are fundamental in the food-processing industry and Fig. 8(b) shows a thin layer of rice-flour paste mounted between slide and coverslip with no additional treatment (and without adding additional water). The signal was quite low from this, but since it is not living material, there is no objection to using moderately high levels of laser power. The images showed good contrast and it was possible to see a lot of detail in the SHG image, which we interpret as showing regions of starch recrystallization. In 3-D stacks, these were seen to be sheet- or ribbon-like. These samples also showed considerable autofluorescence, which was not uniform but also showed structure, probably reflecting variations in water and lipid content.

4 Discussion

Cellulose is a β 1:4 linked glucan;¹⁶ alternate glucose residues are in reversed orientations, which gives a certain amount of symmetry to the molecule, though the chirality of the glucose means that the symmetry is not complete. [Only the dextro form (D-glucose) is found in plants.] This implies that the tensor $\chi_{ijk}^{2\omega}$, the second-order nonlinear optical susceptibility, will have a low but nonzero value. Starch, on the other hand, is α 1:4 linked,¹⁶ so each glucose molecule in the chain is in the same orientation, making the chain much less symmetrical. One would therefore expect, *a priori*, a much larger value

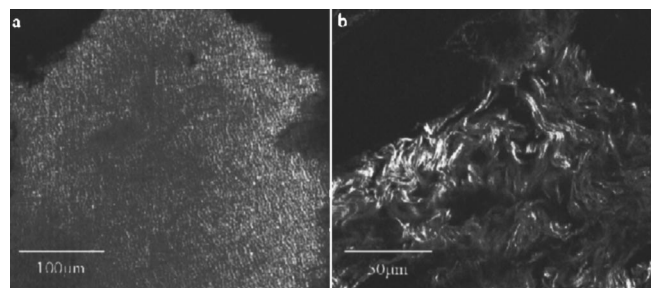


Fig. 8 (a) Fragment of a hand-cut section through a grain of Thai jasmine rice, SHG image at 415 nm, $\times 40$ NA 0.75 dry objective; and (b) rice-flour paste, SHG image at 415 nm, $\times 63$ NA 1.2 water immersion objective.

for the second-order nonlinear optical susceptibility. This implies that starch would be a better generator of the SH than cellulose, and this proves to be the case in practice. Useable images of cellulose in cell walls can be obtained only using high laser power and extended integration times. It is difficult to compare excitation power between polysaccharides of such different structural forms, but the actual laser power after the objective lens was around 75 mW for Fig. 2 (cellulose) and 6 mW for Fig. 7 (starch).

Cheng et al.¹⁸ showed that plant chloroplasts are very susceptible to damage from femtosecond titanium-sapphire laser irradiation. They used 760-nm excitation, substantially shorter than the 830 or 840 nm used here, and found that even a single 3.3-s scan or a small area, under their imaging conditions, could be sufficient to reduce the red fluorescence of chlorophyll, leaving residual green fluorescence. Three such scans were sufficient to cause cytochemically demonstrable cell damage. Similar damage is often observed using blue excitation, so it seems the difference is in degree rather than kind of damage. Successful imaging of living plant cells in a physiologically normal state will therefore depend on minimizing dose, though one could also expect that longer excitation wavelengths than 760 nm would also reduce the extent of the damage.

Our results presented here suggest that imaging without damage will not be achieved when imaging cell walls by SHG from cellulose. High laser powers and long accumulation times were needed to obtain useful images (Figs. 1 and 2). Lignification of the cell wall seemed to increase the SH yield in *Lantana* (Fig. 3), though not in *Apium* (Fig. 1). In both cases, the doses used were far too high to maintain chloroplast viability. It does seem possible that the longer wavelengths given by a chromium forsterite laser¹¹ might increase SH yield from cellulose and reduce the extent of chlorophyll photodamage. The inevitable fact remains that, in spite of its high crystallinity, the β 1:4 structure of the cellulose chain makes it less than optimal for SHG imaging.

Starch, on the other hand, is also crystalline and structurally a much better harmonic generator (Fig. 5). The signal also reveals the orientation of the starch molecules in the grain. Useful signals are obtained at low excitation doses, and as Figs. 6 and 7 show, images of starch can be obtained simultaneously with TPF images of chloroplasts under conditions that show no sign of impacting on cell viability. No loss of red chlorophyll signal was observed in the course of collecting a 97-slice stack; the chlorophyll fluorescence showed no sign of shifting to the green and therefore appearing in the "cell wall" channel in this series. The use of a longer excitation wavelength probably helped in this regard, but the optimized collection geometry of our nondescanned backscatter detectors was probably also a significant factor. Cheng et al.¹⁸ did not mention any nondescanned detection system, so by implication, were probably using the confocal detector system of their Olympus microscope; this will always lead to a severe reduction in collection efficiency compared to wide-field detection. Also, the air spaces in the *Arabidopsis* leaves used had been flooded with water,¹⁸ possibly compromising normal physiological functioning.

Processing of starchy foods for consumption, in its simplest form, consists of breaking down crystalline starch into an amorphous form that is more hydrophilic, more digestible,

and more palatable. This process is referred to (confusingly) as gelatinization in the food processing industry. Subsequent recrystallization (retrogradation) causes defects in products such as lumpiness in sauces and staling of bread.¹⁹ Preventing this to extend shelf life and improve product texture is a key goal of food technology. Since the strength of the SH signal is strongly dependent on crystallinity, SHG microscopy promises to be a very effective tool for imaging this process. Polarized-light wide-field microscopy will also reveal crystalline regions, but does not offer spatial resolution in the axial direction. With SHG microscopy, the structure and extent or retrograded regions can be investigated in all three spatial dimensions.

5 Conclusions

Recently, there has been substantial interest in using harmonic microscopy to study structural proteins in animal tissues,^{9,12} but its potential in the plant world has been underappreciated. To the best of our knowledge, this is only the third paper published in this field. In principle, several polysaccharides could act as sources of SH signals, but only starch and cellulose typically occur in highly crystalline states. Cellulose is a rather weak SH generator, and the incident energy required to give useable signals is likely to be damaging to living cells in many cases. Starch, on the other hand, is easily detected and imaged in three dimensions under conditions that seem not to damage live tissues. Once the crystalline structure has been degraded in food preparation, somewhat higher laser fluences are required, but the material is no longer so susceptible to damage, and extended imaging seemed to make no difference to the sample. This provides agricultural scientists and food technologists with a useful tool for assessing crystal structure and orientation in starchy foodstuffs.

Acknowledgments

Much of this work was carried out while GC was on sabbatical at the Instituto Gulbenkian de Ciência, and we thank the University of Sydney for a Special Studies Program grant and the IGC for making space and facilities available. We are very grateful to Professor Les Copeland and Ms. Chiming (Mary) Tang for the starch paste sample. We thank Nuno Moreno for assistance with, and maintenance of, the multiphoton microscope at the IGC and Eleanor Kable for performing the same services at the Electron Microscope Unit (EMU).

References

1. W. D. Bauer, "Plant cell walls," in *The Molecular Biology of Plant Cells*, H. Smith, Ed., pp. 6–23, Blackwell Scientific Publications, Oxford (1977).
2. R. Bergfeld, V. Speth, and P. Schopfer, "Reorientation of microfibrils and microtubules at the outer epidermal wall of maize coleoptiles during auxin-mediated growth," *Bot. Acta* **101**, 31–41 (1987).
3. L. K. Whiffen, T. P. Dibbayawan, and R. L. Overall, "High-resolution microscopy of cell wall formation in regenerating *Mougeotia* (Chlorophyceae) protoplasts," *Eur. J. Phycol.* **37**, 339–347 (2002).
4. R. C. Carolin, S. W. L. Jacobs, and M. L. Veski, "The structure of the cells of the mesophyll and parenchymatous bundle sheath of the Gramineae," *Bot. J. Linnean Soc.* **66**, 259–275 (1973).
5. M. D. Hatch and N. K. Boardman, "Photosynthesis," in *The Biochemistry of Plants*, Vol. 8, Academic Press, New York (1981).
6. B. E. Juniper, "The perception of gravity by a plant," *Proc. R. Soc. London, Ser. B* **199**, 537–550 (1977).

7. G. Mizutani, Y. Sonoda, H. Sano, M. Sakamoto, T. Takahashi, and S. Ushioda, "Detection of starch granules in a living plant by optical second harmonic microscopy," *J. Lumin.* **87**, 824–826 (2000).
8. J. N. Gannaway and C. J. R. Sheppard, "Second harmonic imaging in the scanning optical microscope," *Opt. Quantum Electron.* **10**, 435 (1978).
9. G. Cox, E. Kable, A. Jones, I. Fraser, F. Manconi, and M. Gorrell, "3-dimensional imaging of collagen using second harmonic generation," *J. Struct. Biol.* **141**, 53–62 (2003).
10. G. Cox and C. Sheppard, "Practical limits of resolution in confocal and non-linear microscopy," *Microsc. Res. Tech.* **63**, 18–22 (2004).
11. S.-W. Chu, I.-H. Chen, T.-M. Liu, P. C. Chen, and C.-K. Sun, "Multimodal nonlinear spectral microscopy based on a femtosecond Cr:forsterite laser," *Opt. Lett.* **26**, 1909–1911 (2001).
12. G. C. Cox, F. Manconi, and E. Kable, "Second harmonic imaging of collagen in mammalian tissue," *Proc. SPIE* **4620**, 148–156 (2002).
13. G. P. Majumdar and R. D. Preston, "The fine structure of collenchyma cells in *Heracleum sphondylium* L.," *Proc. R. Soc. London, Ser. B* **130**, 201–205 (1941).
14. M. Beer and G. Setterfield, "Fine structure in thickened primary walls of celery petioles," *Am. J. Bot.* **45**, 571–580 (1958).
15. J.-C. Roland, "Infrastructure des membranes du collenchyme," *Compt. Acad. Sci. (Paris)* **259**, 4331–4334 (1964).
16. F. A. L. Clowes and B. E. Juniper, *Plant Cells*, Blackwell Scientific, Oxford and Edinburgh (1968).
17. G. C. Cox and B. E. Juniper, "High-voltage electron microscopy of whole, critical-point dried plant cells—fine cytoskeletal elements in the moss *Bryum tenuisetum*," *Protoplasma* **115**, 70–80 (1983).
18. P.-C. Cheng, B.-L. Lin, F.-J. Kao, M. Gu, M.-G. Xu, Z. Gan, M.-K. Huang, and Y.-S. Wang, "Multiphoton fluorescence microscopy—the response of plant cells to high-intensity illumination," *Micron* **32**, 661–669 (2001).
19. X. Liang, J. M. King, and F. H. Shih, "Pasting property differences of commercial and isolated rice starch with added lipids and β -cyclodextrin," *Cereal Chem.* **79**, 812–818 (2002).